Journal of Power Sources 195 (2010) 457–460

Contents lists available at ScienceDirect

Journal of Power Sources

journal homepage: www.elsevier.com/locate/jpowsour

Short communication

Low-cost and durable catalyst support for fuel cells: Graphite submicronparticles

Sheng Zhang[a,b], Yuyan Shao[b], Xiaohong Li[b], Zimin Nie[b], Yong Wang[b], Jun Liu[b], Geping Yin[a,*], Yuehe Lin[b,*]

[a] School of Chemical Engineering & Technology, Harbin Institute of Technology, Harbin 150001, China
[b] Pacific Northwest National Laboratory, Fundamental Science Division, 902 Battelle Boulevard, Richland, WA 99352, USA

ARTICLE INFO

Article history:
Received 19 June 2009
Received in revised form 3 August 2009
Accepted 8 August 2009
Available online 15 August 2009

Keywords:
Polymer electrolyte membrane fuel cell
Electrocatalyst
Graphite submicronparticle
Carbon nanotubes
Durability

ABSTRACT

Low-cost graphite submicronparticles (GSP) are employed as a possible catalyst support for polymer electrolyte membrane (PEM) fuel cells. Platinum nanoparticles are deposited on Vulcan XC-72 carbon black (XC-72), carbon nanotubes (CNT), and GSP via ethylene glycol (EG) reduction method. The morphologies and the crystallinity of Pt/XC-72, Pt/CNT, and Pt/GSP are characterized with X-ray diffraction and transmission electron microscope, which shows that Pt nanoparticles (~3.5 nm) are uniformly dispersed on supports. Pt/GSP exhibits the highest activity towards oxygen-reduction reactions. The durability study indicates that Pt/GSP is 2–3 times durable than Pt/CNT and Pt/XC-72. The enhanced durability of Pt/GSP catalyst is attributed to the higher corrosion resistance of graphite submicronparticles, which results from higher graphitization degree of GSP support. Considering its low production cost, graphite submicronparticles are promising electrocatalyst support for fuel cells.

1. Introduction

There are two main obstacles for the commercialization of proton exchange membrane (PEM) fuel cells: one is the prohibitive production cost, the other is the unacceptable short service lifetime [1]. Correspondingly, the requirements for PEM fuel cell materials are low-cost and high durability. Electrocatalysts play an important role in lowering the cost and improving the lifetime of PEM fuel cells [2]. Recently, the investigations of electrocatalyst durability and the strategies to improve its durability have become a hot topic in fuel cell community [2–4]. Two strategies are usually employed to improve the electrocatalyst durability: to alloy Pt with other transition metals [3] and to develop durable catalyst supports [5].

Carbon materials with high specific surface area and high conductivity are still the key electrocatalyst supports. The most widely used one is Vulcan XC-72 carbon black. Several kinds of new carbon have been developed as alternative support materials for fuel cell catalysts [5]. Carbon nanotubes have been widely investigated as a promising catalyst support [6–11], which exhibit better performance in terms of catalytic activity and durability than the conventional Vulcan XC-72 [12]. Carbon nanotubes are usually functionalized in order to obtain a high dispersion of Pt nanoparticle which is the prerequisite for high catalytic activity. The functionalization of carbon nanotubes usually involves the oxidation with strong acids [13], which is not an environmental benign process and produces defects that will reduce the electrical conductivity and corrosion resistance of carbon nanotubes. The other issue is the high price of carbon nanotubes as compared with conventional carbon black [5,14]. Carbon nanofibers [15], mesoporous carbon [16,17], carbon nanosphere [18,19] are also developed as catalyst supports. These materials have the same cost issue as carbon nanotubes [5].

Here, we reported graphite submicronparticles as a catalyst support for PEM fuel cells. Graphite is widely used in industries and its processing techniques are well developed. The low price of graphite is attractive due to its mass production capability and abundant resources on the earth.

2. Experimental

2.1. Chemicals and materials

Graphite powder (<45 μm, 99.99%) was obtained from Sigma–Aldrich and was attrition milled in isopropanol to an average particle size of 0.2–0.3 μm, which we call graphite submicronparticles (GSP). COOH functionalized multiwall carbon nanotubes(1.8% COOH groups, 10–20 nm in outer diameter, 10–30 m in length, Cheap-Tubes, USA) were used as received. Ethylene glycol (EG), hexachloroplatinic acid ($H_2PtCl_6{\cdot}6H_2O$) and 5 wt.% Nafion solution were obtained from Sigma–Aldrich.

2.2. Catalysts preparation

The 20 wt.% Pt/GSP catalysts were synthesized with ethylene glycol (EG) reduction method developed by Li et al. [9] with some

* Corresponding author. Tel.: +1 509 371 6241, +86 451 86413707.
E-mail addresses: yingphit@hit.edu.cn (G. Yin), yuehe.lin@pnl.gov (Y. Lin).

0378-7753/$ – see front matter © 2009 Elsevier B.V. All rights reserved.
doi:10.1016/j.jpowsour.2009.08.012

modification. Typically, 2.656 mL of hexachloroplatinic acid EG solution (7.53 mg Pt per mL EG) was added drop by drop into 50 mL EG solution with mechanical stirring for 10 min. NaOH (1 M in EG solution) was added to adjust the pH of the solution to above 13. Then 80 mg of GSP was added to the above solution and stirred for 60 min. The solution was heated in refluxing conditions at 130 °C for 4 h to ensure that Pt was completely reduced. After cooling down, the pH of the reaction solution was adjusted to pH < 2 with nitric acid solution, which promotes the adsorption of the suspended metal nanoparticles onto the carbon support, then 20 mL water was added and stirred for 48 h. The resulting catalyst was washed with ultrapure water (18.2 MΩ cm, Mill-Q Corp.) until Cl^- was not detected and then dried overnight at 90 °C in vacuum. Pt/CNT and Pt/XC-72 were prepared in the same way.

2.3. Materials characterization

The catalysts were characterized with transmission electron microscopy (TEM) and X-ray diffraction (XRD). The TEM images of the catalysts were taken in a JEOL TEM 2010 microscope equipped with an Oxford ISIS system. The operating voltage on the microscope was 200 keV. All images were digitally recorded with a slow-scan CCD camera. XRD patterns were obtained using a Philips Xpert X-ray diffractometer using Cu Kα radiation at λ = 1.541 Å.

2.4. Electrochemical measurements

The electrochemical tests were carried out in a standard three-electrode system controlled with a CHI660C station (CH Instruments, Inc., USA) with Pt foil and Hg/Hg_2SO_4 as the counter electrode and reference electrode, respectively. The working electrodes were prepared by applying catalyst ink onto the pre-polished glass carbon disk electrodes. In brief, the catalyst was dispersed in ethanol and ultrasonicated for 15 min to form a uniform catalyst ink (2 mg mL^{-1}). 7.5 μL well-dispersed catalyst ink was applied onto the pre-polished glassy carbon (GC) disk electrode (5 mm in diameter). After dry at room temperature, 2× 5 μL 0.05% Nafion solution was applied onto the surface of the catalyst layer to form a thin protecting. The well-prepared electrodes were dried at room temperature overnight before electrochemical tests. The total loading of catalyst was 15 μg (3 μg Pt).

The working electrodes were first activated with cyclic voltammograms (CV, 0–1.1 V at 50 mV s^{-1}) in N_2-purged 0.5 M H_2SO_4 solution until a steady CV was obtained. The linear sweep voltammograms (LSV) for oxygen-reduction reaction (ORR) is measured with a Pine rotator system (Pine Instruments Company, USA) in oxygen-saturated 0.5 M H_2SO_4 solution (10 mV s^{-1}). The background current was measured similarly in an N_2 atmosphere without rotation. The durability tests catalysts were done in N_2-saturated 0.5 M H_2SO_4 solution with potential step method (1.4 V_10 s–0.85 V_5 s) [20]. Before and after the degradation test, CV in N_2-purged 0.5 M H_2SO_4 solution and LSV in O_2-saturated 0.5 M H_2SO_4 solution were measured.

All the tests were conducted at room temperature. All potentials were reported versus reversible hydrogen electrode (RHE).

3. Results and discussions

3.1. Catalysts characterizations

Fig. 1 shows the TEM images and Pt nanoparticle size distribution histograms of Pt/XC-72, Pt/CNT, and Pt/GSP. Pt nanoparticles were uniformly dispersed on the three supports. The number-averaged diameters ($\bar{d}_n$) of the Pt nanoparticles can be calculated from TEM images using the following equation:

$$\bar{d}_n = \frac{\sum_{i=1}^{n} d_i}{n} \quad (1)$$

The value of $\bar{d}_n$ is 2.2, 2.3, and 2.2 nm for Pt/XC-72, Pt/CNT, and Pt/GSP, respectively. This can be considerably different from the volume/area averaged diameter ($\bar{d}_{v/a}$), which is calculated with the following equation:

$$\bar{d}_{v/a} = \frac{\sum_{i=1}^{n} d_i^3}{\sum_{i=1}^{n} d_i^2} \quad (2)$$

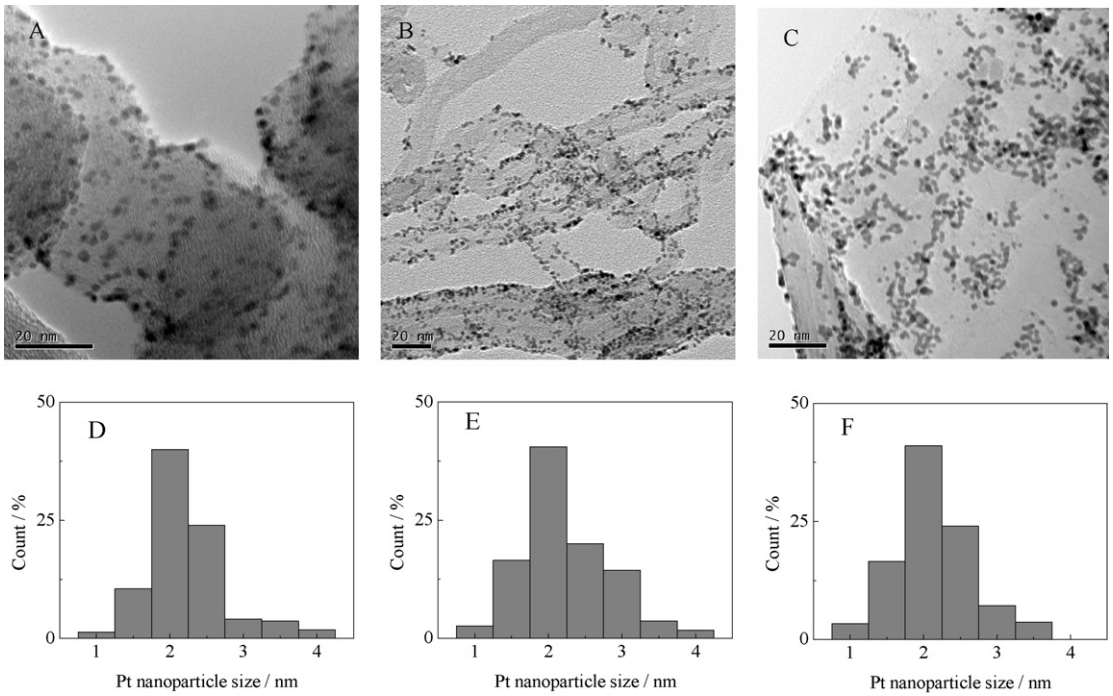

Fig. 1. TEM images and Pt nanoparticle size distribution histograms of Pt/XC-72 (A and D), Pt/CNT (B and E), and Pt/GSP (C and F).

It is generally believed that the volume/area averaged diameter ($\bar{d}_{v/a}$) better represents the specific surface area of platinum than the number-averaged diameter [21]. The results show that the values of $\bar{d}_{v/a}$ in Pt/XC-72, Pt/CNT, and Pt/GSP are 3.3, 3.6, and 3.5 nm, respectively.

The XRD patterns of Pt/XC-72, Pt/CNT, and Pt/GSP are shown in Fig. 2, which indicates the presence of Pt nanoparticles on these samples [22]. The C(0 0 2) diffraction peaks occur at $2\theta = 26.5^\circ$ and $2\theta = 25.9^\circ$ for Pt/GSP and Pt/CNT, respectively, with the former much sharper and narrower, indicating a more ordered graphitic structure for graphite submicronparticles in Pt/GSP [14]. For Pt/XC-72, C(0 0 2) diffraction peak was greatly suppressed, indicating much lower graphitic structure of XC-72 carbon black. Furthermore, the peak at $2\theta = 55.3^\circ$ for Pt/GSP is ascribed to C(0 0 4) diffraction, which is indicative of high crystallinity of the carbon structure [14,23]. These results indicate that GSP has the highest graphitization degree of the three samples, which implies the high electrical conductivity of GSP [24,25].

The reaction and size control mechanism of the EG reduction method in the synthesis of Pt nanocatalysts has been thoroughly investigated by Bock et al. [26]. During the reduction of Pt salt (to Pt metal), ethylene glycol is oxidized and produces glycolate anion (at high pH). The stabilizing effect of glycolate anion directly relates to the pH of the solution. In neutral and acidic solution, glycolate anion forms glycolic acid, which is a poor stabilizer for Pt colloid. The high pH (>12) ensures the deprotonation of glycolic acid to form glycolate anion as a strong stabilizer for the Pt colloids, and results in small and uniformly dispersed Pt particles, as can be seen from the above TEM images and XRD analysis.

3.2. Electrochemical properties

Fig. 3 shows the cyclic voltammograms (CV) in N_2-saturated acid solution on Pt/XC-72, Pt/CNT, and Pt/GSP. Typical hydrogen and oxygen adsorption/desorption behavior on platinum can be obviously observed on these samples. Electrochemical surface area (ESA) of platinum can be calculated with coulombic charges accumulated during hydrogen adsorption and desorption. The values of ESA are 52.2, 49.5, and 50.2 $m^2\,g^{-1}$ Pt for Pt/XC-72, Pt/CNT, and Pt/GSP, respectively. Oxygen-reduction reaction (ORR) activity was measured with linear sweep voltammograms in oxygen-saturated 0.5 M H_2SO_4 solution (10 mV s^{-1}). The oxygen-reduction kinetics were obtained using the well-known mass-transport correction for rotating disk electrodes (Koutecky–Levich equation) [24] and the loading of Pt on electrodes for the three samples is the same (3 μg). Results show that ORR activity at 0.90 V is 17.3, 16.7, and 20.4 A g^{-1} Pt for Pt/XC-72, Pt/CNT, and Pt/GSP, respectively. It can be seen that the ESA are similar for three catalysts, while the oxygen-reduction activity on Pt/GSP is nearly 20% higher than that on Pt/XC-72 and Pt/CNT. The enhanced ORR activity might be due to the higher electrical conductivity of GSP, which results from the more highly ordered graphitic structure as seen in the XRD patterns [9,27,28].

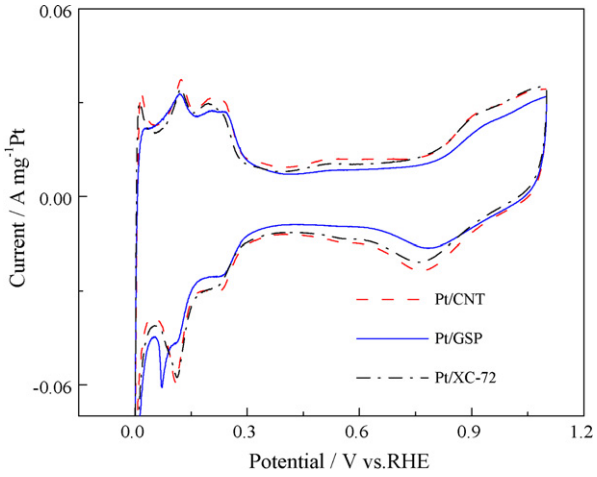

Fig. 3. Cyclic voltammograms (50 mV s^{-1}) of Pt/XC-72, Pt/CNT, and Pt/GSP in N_2-saturated 0.5 M H_2SO_4.

Fig. 4 shows the degraded percentage in ESA and ORR activity of Pt/XC-72, Pt/CNT, and Pt/GSP in the durability test under the condition of potential step (1.4–0.85 V) for 22 h. The potential step method has been shown to be able to effectively study the corrosion of carbon support in our previous paper [20], which is equivalent to the U.S. Department of Energy (DOE) protocol with the fixed-potential holding [1]. It can be seen that the ESA degraded by 58%, 47%, and 32% for Pt/XC-72, Pt/CNT, and Pt/GSP, respectively, and the ORR current at 0.90 V degraded by 57%, 40%, and 19%, respectively. It can be concluded that Pt/GSP electrocatalyst exhibits much higher durability than that of Pt/XC-72 and Pt/CNT. Since our durability test protocol focuses on carbon support corrosion [20], it is expected that the enhanced durability of Pt/GSP is due to the higher stability of graphite submicronparticles.

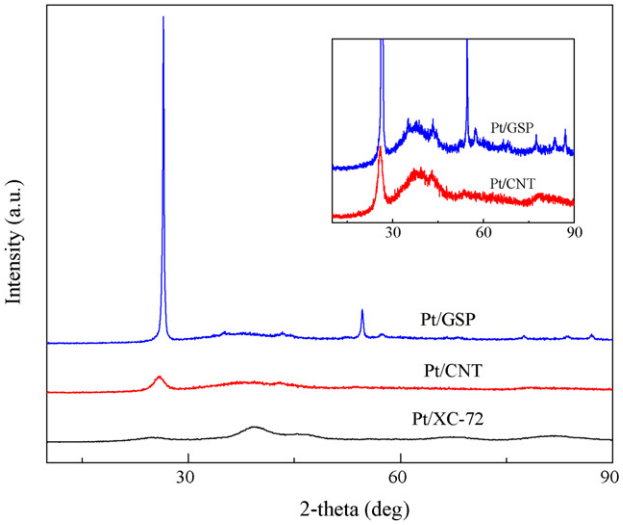

Fig. 2. X-ray diffraction patterns of Pt/XC-72, Pt/CNT, and Pt/GSP.

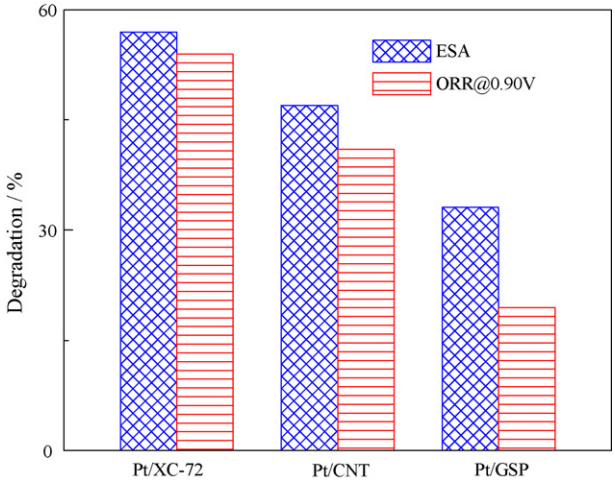

Fig. 4. The degraded percentage in ESA and ORR activity of Pt/XC-72, Pt/CNT, and Pt/GSP during the durability test under potential step (1.4–0.85 V) for 22 h.

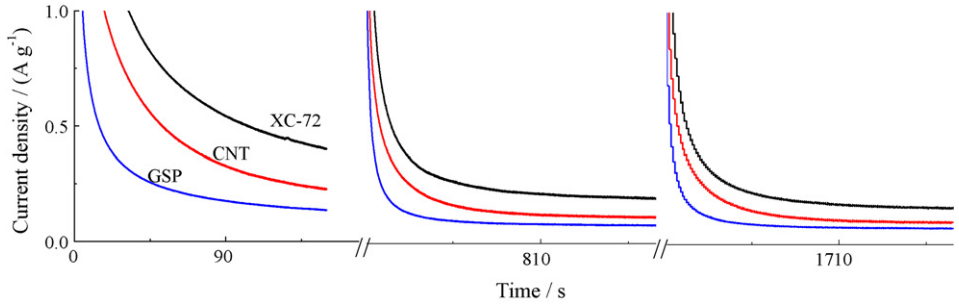

Fig. 5. Amperometric *i*–*t* curves on XC-72, CNT and GSP under the potential step condition (1.4 V_150 s–0.85 V_30 s) (only the oxidation currents at 1.4 V are shown).

Fig. 5 shows the amperometric *i*–*t* curves on XC-72, CNT, and GSP under the potential step (1.4 V_150 s–0.85 V_30 s). It can be seen that the oxidation current of GSP is much lower than that of XC-72 and CNT, indicating that GSP has the most resistance to electrochemical corrosion. As mentioned above (in XRD analysis), graphite submicronparticles exhibit more ordered graphitic structures (higher graphitization degree), which contributes to the enhanced durability [11]. In addition, increasing the degree of graphitization enhances the strength of the delocalized π-sites (sp^2-hybridized carbon) on carbon support, which act as anchoring centers for Pt nanoparticles, thus strengthen the interaction between the Pt nanoparticles and carbon support [29]. As a result, the resistance of Pt nanoparticles to sintering is increased with enhancing the degree of graphitization of the catalyst support.

4. Conclusions

Graphite submicronparticles (GSP) have been prepared from commercial graphite and demonstrated as a promising catalyst support for PEM fuel cells. Highly dispersed Pt nanoparticles were deposited via ethylene glycol (EG) reduction method on XC-72 carbon black, carbon nanotubes, and GSP. Pt/GSP exhibits an enhanced activity towards oxygen-reduction and a much higher durability than Pt/XC-72 and Pt/CNT. These are attributed to the highly ordered graphitic structure of GSP. The total synthesis process of catalysts does not involve environmental-unfriendly chemicals. This provides an environmental benign and low-cost approach for developing durable catalysts for PEM fuel cells.

Acknowledgments

This work is partially supported by the Natural Science Foundation of China (Nos. 50872027 and 20606007) and partially by the U.S. DOE-EERE Hydrogen Program. Part of the research described in this paper was performed at the Environmental Molecular Sciences Laboratory, a national scientific-user facility sponsored by the U.S. Department of Energy's (DOE's) Office of Biological and Environmental Research and located at Pacific Northwest National Laboratory. PNNL is operated for DOE by Battelle under Contract DE-AC05-76L01830. The authors would like to acknowledge Dr. Chongmin Wang for TEM measurements. Sheng Zhang would like to acknowledge the fellowship from the China Scholarship Council to work at PNNL.

References

[1] R. Borup, J. Meyers, B. Pivovar, Y.S. Kim, R. Mukundan, N. Garland, D. Myers, M. Wilson, F. Garzon, D. Wood, P. Zelenay, K. More, K. Stroh, T. Zawodzinski, J. Boncella, J.E. McGrath, M. Inaba, K. Miyatake, M. Hori, K. Ota, Z. Ogumi, S. Miyata, A. Nishikata, Z. Siroma, Y. Uchimoto, K. Yasuda, K.I. Kimijima, N. Iwashita, Chem. Rev. 107 (2007) 3904–3951.
[2] Y.Y. Shao, G.P. Yin, Y.Z. Gao, J. Power Sources 171 (2007) 558–566.
[3] J. Zhang, K. Sasaki, E. Sutter, R.R. Adzic, Science 315 (2007) 220–222.
[4] Y. Shao-Horn, W.C. Sheng, S. Chen, P.J. Ferreira, E.F. Holby, D. Morgan, Top. Catal. 46 (2007) 285–305.
[5] Y. Shao, J. Liu, Y. Wang, Y. Lin, J. Mater. Chem. 19 (2009) 46–59.
[6] G. Girishkumar, K. Vinodgopal, P.V. Kamat, J. Phys. Chem. B 108 (2004) 19960–19966.
[7] Y. Lin, X. Cui, C. Yen, C.M. Wai, J. Phys. Chem. B 109 (2005) 14410–14415.
[8] Y. Lin, X. Cui, C. Yen, C.M. Wai, Langmuir 21 (2005) 11474–11479.
[9] W.Z. Li, C.H. Liang, W.J. Zhou, J.S. Qiu, Z.H. Zhou, G.Q. Sun, Q. Xin, J. Phys. Chem. B 107 (2003) 6292–6299.
[10] G. Wu, L. Li, J.H. Li, B.Q. Xu, J. Power Sources 155 (2006) 118–127.
[11] J.J. Wang, G.P. Yin, Y.Y. Shao, Z.B. Wang, Y.Z. Gao, J. Phys. Chem. C 112 (2008) 5784–5789.
[12] X. Wang, W.Z. Li, Z.W. Chen, M. Waje, Y.S. Yan, J. Power Sources 158 (2006) 154–159.
[13] Y.C. Xing, J. Phys. Chem. B 108 (2004) 19255–19259.
[14] P.V. Shanahan, L.B. Xu, C.D. Liang, M. Waje, S. Dai, Y.S. Yan, J. Power Sources 185 (2008) 423–427.
[15] E.S. Steigerwalt, G.A. Deluga, D.E. Cliffel, C.M. Lukehart, J. Phys. Chem. B 105 (2001) 8097–8101.
[16] H. Chang, S.H. Joo, C. Pak, J. Mater. Chem. 17 (2007) 3078–3088.
[17] F.B. Su, J.H. Zeng, X.Y. Bao, Y.S. Yu, J.Y. Lee, X.S. Zhao, Chem. Mater. 17 (2005) 3960–3967.
[18] Y.Y. Song, Y. Li, X.H. Xia, Electrochem. Commun. 9 (2007) 201–205.
[19] Z.H. Wen, Q. Wang, Q. Zhang, J.H. Li, Electrochem. Commun. 9 (2007) 1867–1872.
[20] Y.Y. Shao, R. Kou, J. Wang, V.V. Viswanathan, J.H. Kwak, J. Liu, Y. Wang, Y.H. Lin, J. Power Sources 185 (2008) 280–286.
[21] P.J. Ferreira, G.J. la, O.Y. Shao-Horn, D. Morgan, R. Makharia, S. Kocha, H.A. Gasteiger, J. Electrochem. Soc. 152 (2005) A2256–A2271.
[22] G. Wu, B.Q. Xu, J. Power Sources 174 (2007) 148–158.
[23] T.W. Kim, I.S. Park, R. Ryoo, Angew. Chem. -Int. Ed. 42 (2003) 4375–4379.
[24] D. Pantea, H. Darmstadt, S. Kaliaguine, L. Summchen, C. Roy, Carbon 39 (2001) 1147–1158.
[25] D. Pantea, H. Darmstadt, S. Kaliaguine, C. Roy, Appl. Surf. Sci. 217 (2003) 181–193.
[26] C. Bock, C. Paquet, M. Couillard, G.A. Botton, B.R. MacDougall, J. Am. Chem. Soc. 126 (2004) 8028–8037.
[27] A. Kongkanand, K. Vinodgopal, S. Kuwabata, P.V. Kamat, J. Phys. Chem. B 110 (2006) 16185–16188.
[28] P.J. Britto, K.S.V. Santhanam, A. Rubio, J.A. Alonso, P.M. Ajayan, Adv. Mater. 11 (1999) 154–157.
[29] J. Lu, I. Do, L.T. Drzal, R.M. Worden, I. Lee, ACS Nano 2 (2008) 1825–1832.